

Geospatial Detection of Hidden Lithologies along Taiping to Ipoh Stretch of the Highway Using Medium Resolution Satellite Imagery in Malaysia

Idris Bello Yamusa¹, Mohd Suhaili Ismail², Abdulwaheed Tella^{3*}

^{1,2}Petroleum Geoscience Department, University Teknologi PETRONAS, Bandar Seri Iskandar, Perak, Malaysia,

³Geospatial Analysis and Modelling (GAM) Research Laboratory, Department of Civil and Environmental Engineering, Universiti Teknologi PETRONAS (UTP), 32610 Seri Iskandar, Perak, Malaysia.

*Corresponding author: tellaabdulwaheed01@gmail.com

Abstract — A highway that is an essential link to major cities is prone to different geological hazards. The first step to tackling this problem is identifying the type of lithologies underneath the region's bedrock. Detecting lithologies in a tropical rainforest area such as Malaysia may be a difficult task and logistically intricate due to inaccessibility to some areas. To overcome this challenge, band rationing was performed on the surface reflectance band of Landsat 8 OLI in the GIS environment regarding Malaysian locales. Four different band ratios were generated along with composite bands. The band ratios used for this study are $6/5$ $7/6$ $4/7$, $5/4$ $6/5$ $7/6$, $6/7$ $4/2$ $5/4$, and $6/5$ $6/7$ $4/2$. The band ratio $4/2$ is used to map iron oxides due to their absorption capability in the blue region and high reflectance capability in the red region. The band ratio $6/7$ is used for the lithological mapping of clay minerals and kaolinite due to the high and low reflectance in bands 6 and 7, respectively. While band ratio $5/4$ is used for Alteration minerals, and ratio $6/5$ is used for ferrous minerals. The generated outcome shows the lithological combination as granites, limestones, phyllites, and metasandstones. The metasediments and limestones region are also well discriminated within small areas of the study area. The best band ratio of $5/4$ $6/5$ $7/6$ illustrates the most distinct spectral reflectance and absorption capability bringing out the weathered medium-grained granites. A new up-to-date lithologic map of the Taiping to Ipoh area is proposed based on the interpretation of image results and field verification work. Results show that the proposed methods have great potential for lithological mapping of tropical regions. Thus, this technique is recommended for mapping different types of granitic rocks, which is the most abundant rock underlying the study area along the highway.

Keywords - Lithology, Highway, Landslides, Hazards, Band ratioing

©2021 Penerbit UTM Press. All rights reserved.

Article History: Received 22 December 2020, Accepted 13 April 2021, Published 1 August 2021

*How to cite: Yamusa, I.B., Ismail, M.S., Tella, A. (2021). Geospatial Detection of Hidden Lithologies along Taiping to Ipoh Stretch of the Highway Using Medium Resolution Satellite Imagery in Malaysia. Journal of Advanced Geospatial Science & Technology*1(1), 19-37.

1. Introduction

Lithology or rock type is one of the key factors contributing to landslides (Yusof et al., 2015). The geologic environment has a major influence on the possibility, mechanism, and classification of earth movements or hazards that may occur and the strength of potential rupture surfaces in rock and soil. The type of lithology stratigraphy, structure (bedding, jointing, faulting, folding), defects (joints and crushed zones), and weathering are also relevant. The soils developed in these environments and their susceptibility to hazards are related to the underlying rocks (Fell et al., 2012).

The geomorphology of the area consists of an undulating plateau and a hilly terrain. The geology of the area primarily consists of Quaternary and Devonian granite. Many landslides were recorded along PLUS highways, roads, and streams in recent years. The decision upon road construction according to the data and outcome of geological mapping results in a significant reduction of the construction cost with a corresponding increase in construction safety. However, according to Georgiadis et al. (2007), the selection of new road over an old road is because an old road section that crosses the mountain range forms artificial slopes of variable orientations and in various geological formations the old road possesses different mechanical characteristics. These enable evaluating different conditions of potential instabilities. It is, therefore, necessary to cross-check the safety of a functioning road.

Many factors trigger hazards such as landslides, including lithology, changes in slope geometry, water level, rainfall intensity, and loading. However, Malaysia's primary cause of landslides is the high amount of rainfall (Sa'adin et al., 2016). Precipitation is absorbed differently by different rocks. Converting a forested area to a place where crops are cultivated can increase the moisture in the soil enough to cause landslide problems (DeGraff and Romesburg, 1980). Constructing a road that cuts off the toe of a steep slope can also increase landslide susceptibility. It is possible to reduce the potential impact of natural landslide activity and reduce development-initiated landslide occurrence by early consideration of these effects (Kockelman, 1986).

2. Geology of Peninsular Malaysia

Three north-south belts characterize the Malay Peninsula: the Western, Central, and Eastern belts (Figure 1). More than 90% of the plutonic rocks in Peninsular Malaysia are granitic. The granitoids can be divided into two belts, a West Malaya Main Range S-Type group of granitoids that yield Late Triassic to earliest Jurassic, and an eastern Malaya group of dominantly I-Type granitoids with a range of ages from early Middle Permian to early Late

Triassic. A significant Late Cretaceous tectono-thermal event affected the Peninsula with major faulting, granitoid intrusion, and re-setting of palaeomagnetic signatures (Metcalf, 2013).

The study area also falls within the Western Belt of Peninsular Malaysia with a main Range S-Type group of granitoids from the Late Triassic to earliest Jurassic periods. There are conjugate sets of brittle fractures affecting the surrounding plutons, one of which is parallel to the cleavage and may reflect the accommodation of deformation at two different structural depths (Sautter et al., 2017). Moreover, the geomorphology of the area consists of hilly terrains and undulating plateaus. The geology of the area mainly consists of Quaternary and Devonian granite. In recent years, many landslides have been recorded along PLUS highways, roads, and streams, which scour the sides of streams (Yusof et al., 2015).

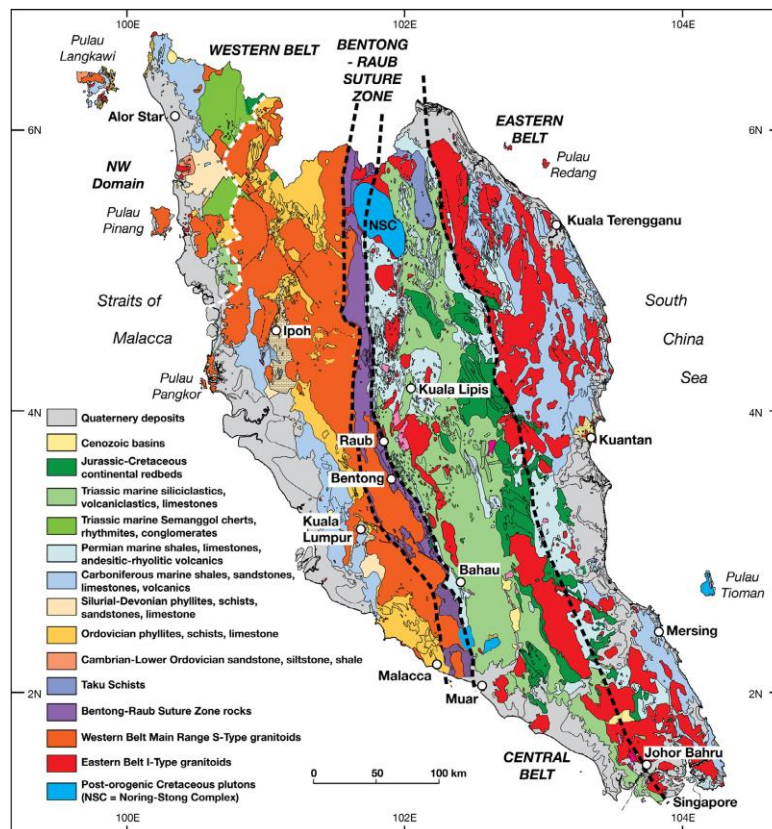


Figure 1. Simplified geological map of the Malay Peninsula. Modified from Metcalfe (2013).

3. The study area

The Taiping to Ipoh stretch of the Highway falls within the North-South Expressway Project (NSE), which is the longest expressway in Malaysia. It has a length of approximately 772 km (482 miles) running from Bukit Kayu Hitam to Johor Bahru (Klia2.info, 2019) and passes seven states, i.e., Johor, Melaka, Negeri Sembilan, Selangor, Perak, Penang, and Kedah. This expressway links many major cities and towns, thus acting as the backbone to the economic development of western Peninsular Malaysia (Ahmad et al., 2016).

The study area (Figure 2) extends from Taiping at 4° 51' N and 101° 43' E of latitude and longitude to Ipoh at 4° 35' N and 101° 04' E of latitude and longitude, having a length of about 73 km. Unexpectedly, according to Yusof et al. (2015), some part of the study area experiences frequent mass movements that cause erosion and landslides.

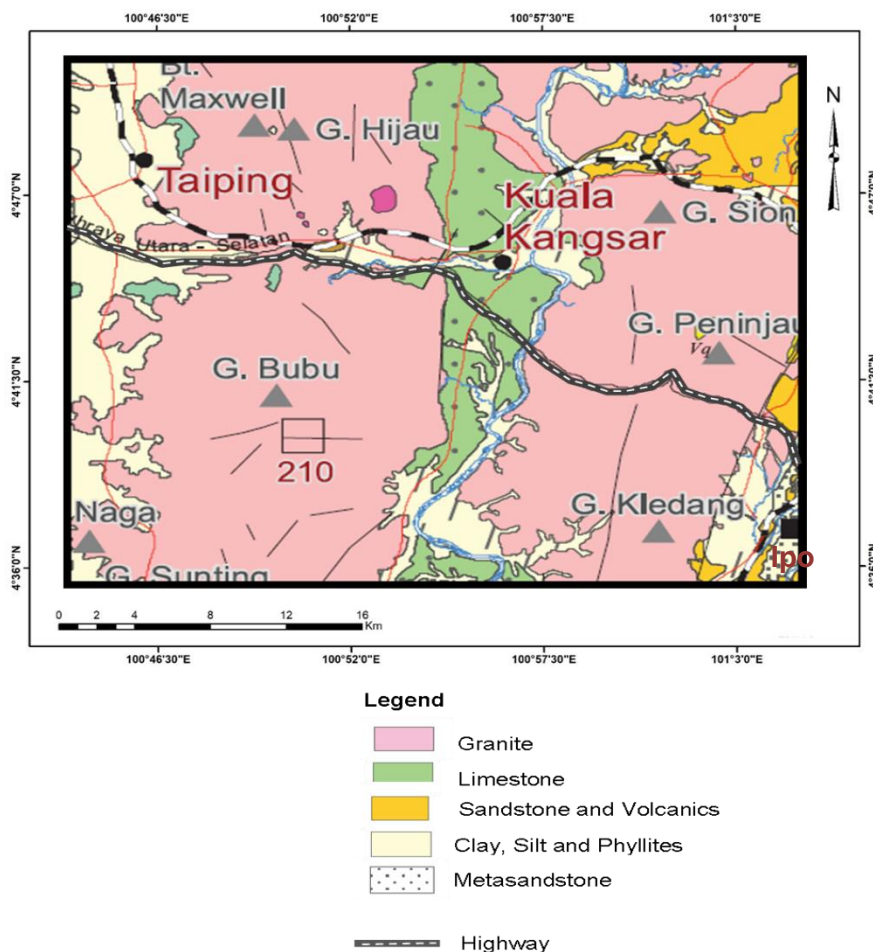


Figure 2. Geologic Map of Study area (source: Directorate of National Mapping, 2014).

4. Aim and objectives

There is scant literature that investigates the characteristics of different lithological features in the study area. Approaches to identify these features through varying spectral reflectance have not been examined due to the dense vegetation in the region. Thus, this study aims to fill this gap by investigating the efficacy of remote sensing applications in lithological mapping using remote sensing data and validating the results through fieldwork. This approach will also serve as the first step to developing any model on engineering and geological works along the highway suitable for large-scale exploration. In addition, this study will promote a better understanding of different landforms in the area, which may influence geological hazards such as landslides. Lastly, this research aims to provide more comprehensive data exploration on lithology, deformation via determination of best band combination, and a digital elevation model of the study area.

Land use is the land cover of an area due to human activities. In general, the study area is highly vegetated, and quite a large portion of it is inaccessible. The classification of land use is shown in Table 1.

Table 1. Land Use Classification

Distinct Lands
1. Agricultural Land
2. Barren Land
3. Moderately Vegetated Area
4. Sparsely Vegetated Area with Less Ground Cover
5. Urban Area
6. Water Body
7. Thickly Vegetated Area

5. Materials and methods

Topographic map sheets were obtained and combined to cover the entire stretch of the highway, and it was traced out using ArcGIS 10.7. The Digital Elevation Model of the study area was downloaded from Shuttle Radar Topography Mission (SRTM) data in Raster form (Figure 4). It was imported to ArcGIS 10.7, where the DEM was extracted, and the highway stretch was traced. For the band ratioing, Landsat 8 OLI Surface Reflectance, ENVI 5.3, and ArcGIS 10.7 was used.

The rationing was done in the ENVI 5.3 software, whereas the composite bands were generated in ArcGIS 10.7.

Table 2. Attributes of Landsat 8 OLI (source: USGS,2020)

Bands	Meaning	Wavelength (μm)	Spatial Resolution (meter)
Band 1	Coastal / Aerosol	0.433 to 0.453	30
Band 2	Visible blue	0.450 to 0.515	30
Band 3	Visible green	0.525 to 0.600	30
Band 4	Visible red	0.630 to 0.680	30
Band 5	Near-infrared	0.845 to 0.885	30
Band 6	Short wavelength infrared	1.56 to 1.66	30
Band 7	Short wavelength infrared	2.10 to 2.30	30
Band 8	Panchromatic	0.50 to 0.68	15
Band 9	Cirrus	1.36 to 1.39	30
Band 10	Long wavelength infrared	10.3 to 11.3	100
Band 11	Long wavelength infrared	11.5 to 12.5	100

Using statistical results, the background (threshold) values and, consequently, the expected anomalies of each band ratio image could be obtained according to one of the following equations (Fatima et al., 2017);

$$\text{TH} = \text{M} + 3 * \text{SD} \dots \text{ at confidence } 98\% \quad (1)$$

$$\text{TH} = \text{M} + 2 * \text{SD} \dots \text{ at confidence } 95\% \quad (2)$$

$$\text{TH} = \text{M} + \text{SD} \dots \text{ at confidence } 92\% \quad (3)$$

where,

TH is the threshold pixel value; M is the mean pixel value; SD is the standard deviation.

6. Results

6.1 Topographic map and road assessment

The study area, which is the stretch of the Taiping to Ipoh Highway, exceeds one topographic map. Thus about 79 topographic maps were studied from which three (3) were selected and contained the precise stretch of the highway (Figure 3). These included sheets 3463 Kuala Kangsar, 3562 Ipoh, and 3563 Sungai Siput Utara depicting the Northwestern, Northeastern, and Southeastern parts of the study area. A topographic map was used so that the vegetated, non-vegetated areas, and urban settlements can be correlated with results obtained from band ratio combinations as a guide and means of knowing the recent changes that occurred.

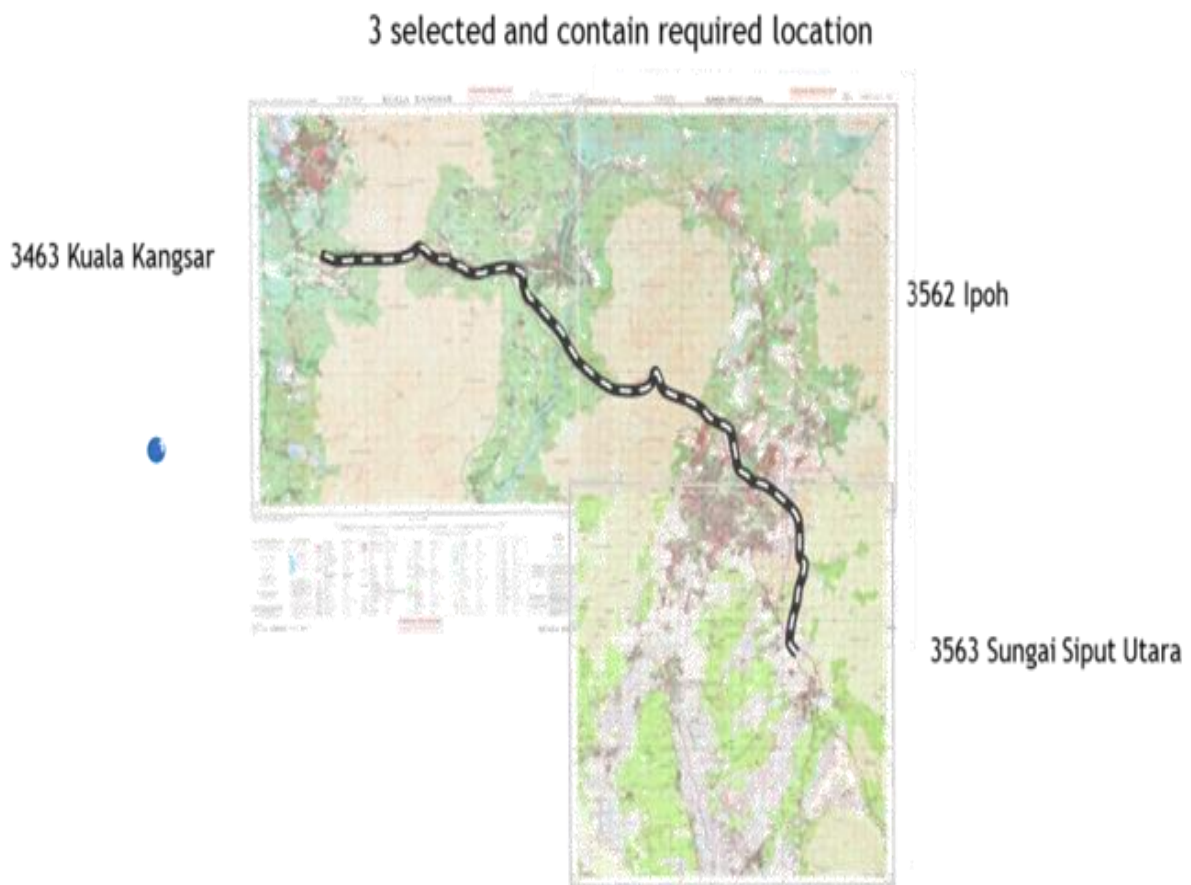


Figure 3. Topographic map of Taiping to Ipoh stretches of the Highway, Series L7030 at Scale 1:50,000 (source: Directorate of National Mapping, Malaysia, 1989 and 2006)

6.2 Digital Elevation Model

The digital elevation model (Figure 4) shows the different heights above sea level depicted by different colors. The highest and lowest points are about 1650ft and -11ft above the sea, respectively. The segment of the highway cuts across areas with generally low elevation but are in contact with high steep slopes. This is one of the dangers the road is exposed to. The areas with the high elevation were found to be granitic.

6.3 Band Ratioing

Band ratioing is an arithmetic method widely utilized in lithological mapping (Adiri et al., 2016). It involves dividing the pixel value of the band by another value (Lillesand et al., 2015). This ensures spectral enhancement, which aids better distinguishing features (Askari et al., 2018). For better visualization, interpretation, and discrimination of lithological units, an RGB color composite was used. The band ratio used for this study was adopted from Adiri et al. (2016), which also aligns with Ourhzif et al. (2019). Table 3 to 6 shows the minimum and maximum value of the pixel cells. The threshold value for each band combination was examined.

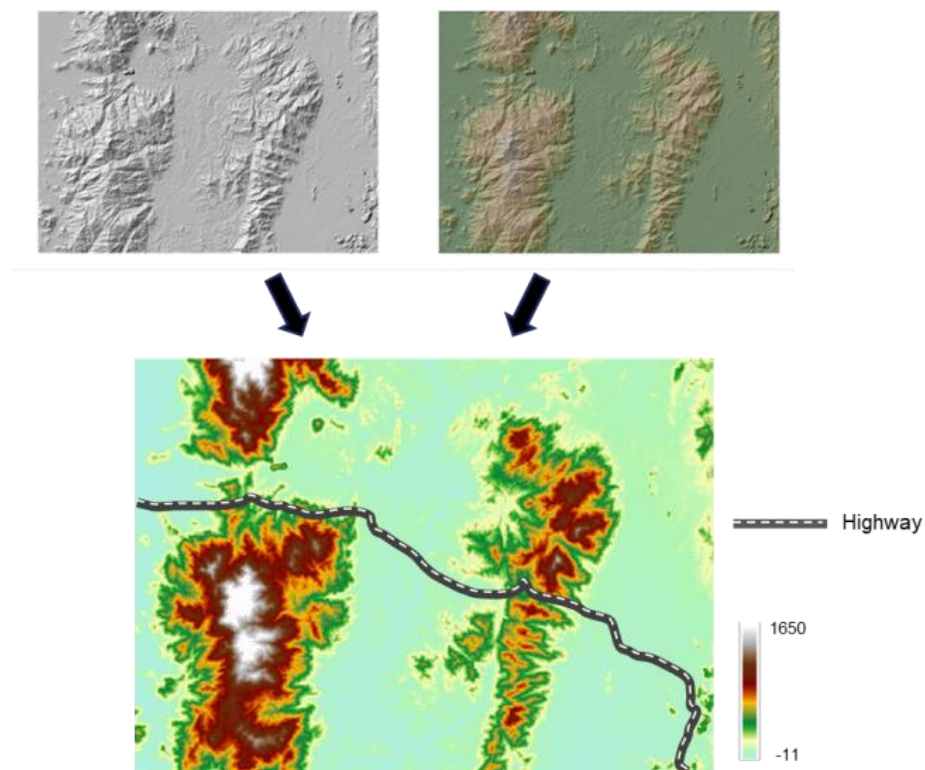


Figure 4. Digital Elevation Model of the study area using SRTM Raster
(source: OpenTopography, 2020)

Image threshold is a common task in remote sensing applications. The image threshold creates a binary representation of the image by classifying the pixels into two categories (dark & light) by Balaji and Sumathi (2014). To determine the threshold values for density slicing and the feature anomalies difference, the formula generated by Fatima et al. (2017) was used. Color composite is created based on the spectral properties of the rock and the alteration of minerals. The color combinations were used to map the clay minerals, kaolinite, and iron oxides. Noteworthy, spectral reflectance analysis is also crucial for selecting spectral bands for remote sensing analysis of inaccessible areas (Ahmad et al., 2016). Thus, the spectral reflectance of the band ratio is considered (Figure 5b, 6b, 7b, and 8b). The band ratio used for this study was adopted from Adiri et al. (2016).

Table 3. The first band combination is 6/5, 7/6, 4/7

Ratio	Min	Max	Mean	St. Dev	Threshold Value	Conf.
B6/B5	0	255	58	60	178	95%
B7/B6	0	255	56	55	166	95%
B4/B7	0	255	115	36	151	92%

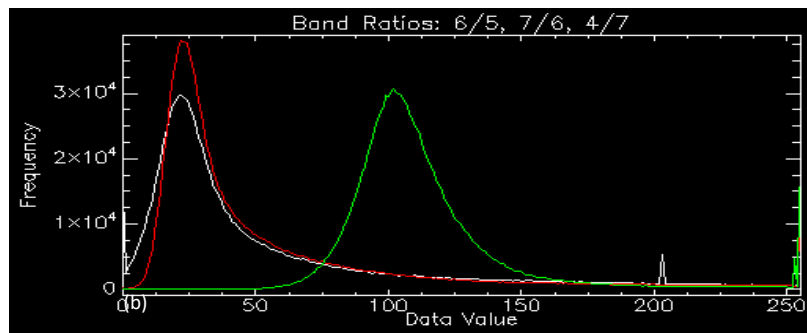
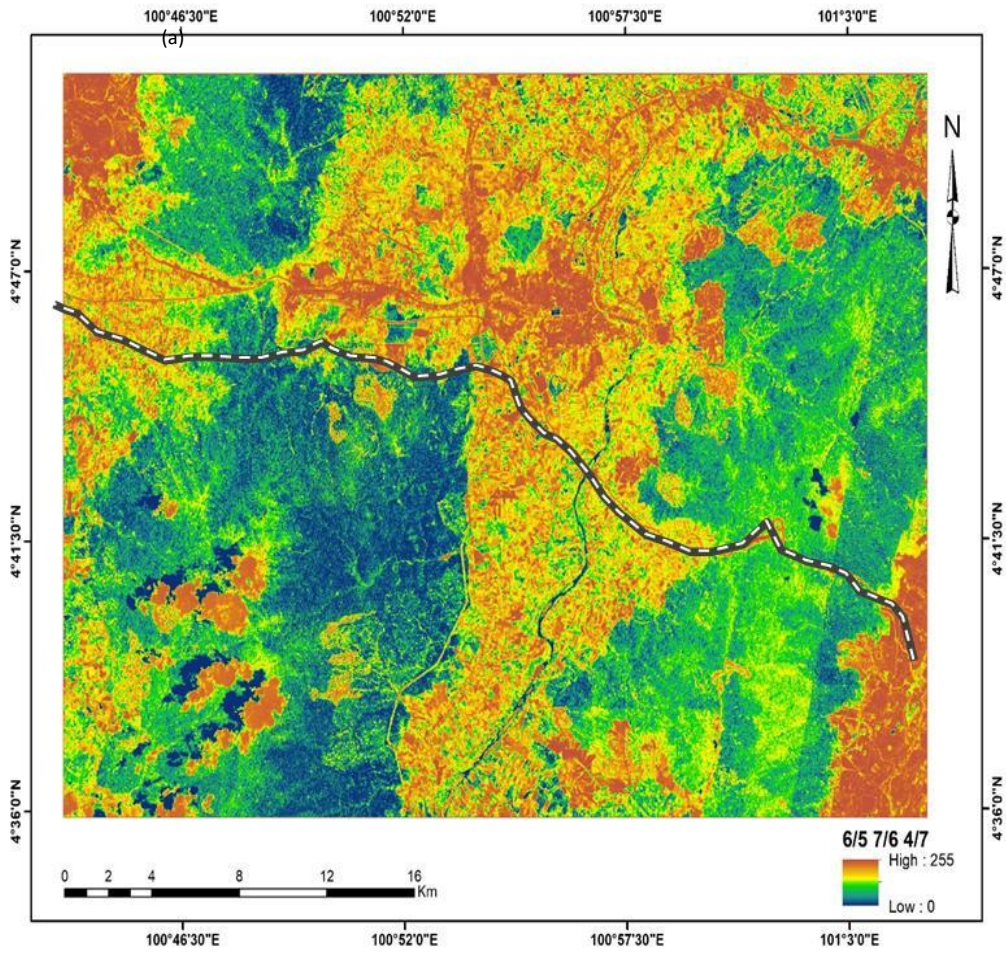


Figure 5. (a) Composite 6/5 7/6 4/7 Bands and (b) Spectral Reflectance

Table 4. Band Ratios 5/4 6/5 7/6

Basic Stats	Min	Max	Mean	Stdev	Threshold Value	Conf.
B5/B4	0	255	150	69	219	92%
B6/B5	0	255	58	60	238	98%
B7/B6	0	255	56	55	221	98%

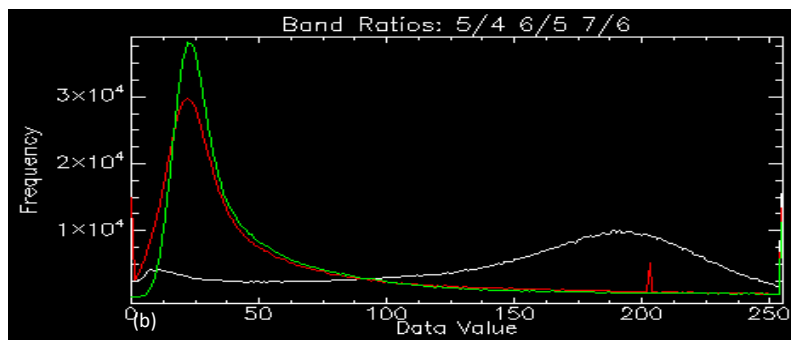
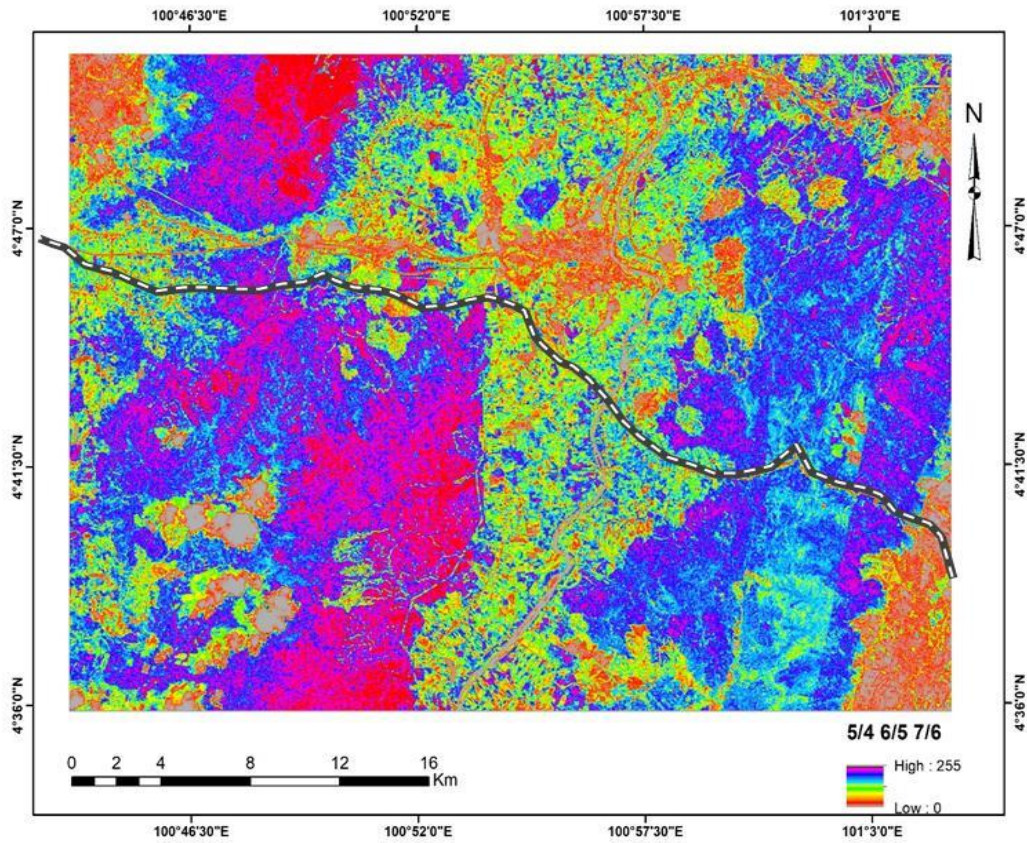


Figure 6. (a) Composite 5/4 6/5 7/6 Bands and (b) Spectral Reflectance

The two band ratios were obtained from Ourhizif et al. (2019). This study asserts that the 4/2 band is used for mapping iron oxides due to its absorption capability in the blue region and high reflectance capability in the red region. Band ratio 6/7 is used for lithological mapping of clay minerals and kaolinite due to the high and low reflectance in bands 6 and 7, respectively. While 5/4 is used for alteration minerals, and ratio 6/5 is suitable for ferrous minerals.

Table 5. The band combination is 6/7, 4/2, 5/4

Basic Stats	Min	Max	Mean	Stdev	Threshold Value	Conf.
B6/B7	0	255	186	64	250	92%
B4/B2	0	255	192	33	225	92%
B5/B4	0	255	150	69	219	92%

7. Discussion

For identifying lithological features using Landsat 8 OLI, the unique spectral reflectance of each feature was selected. This study considered the absorption and reflection of the spectral alteration of the features in the study area. Iron oxides were mapped using bands 2 and 4. This is because iron oxides have high absorption (0.45–0.52 μm) and reflectance (0.63–0.69 μm). Thus, concerning Pour and Hashim (2015), this band ratio is also used to detect iron oxides. Ferrous minerals were mapped by Gupta (2017) using band ratio 6/5 because band 5 has high absorption (0.85–0.89 μm) due to the iron absorption features and high reflectance in and band 5 (1.560–1.660 μm). Clay minerals are best detected using band ratio 6/7 (Mars and Rowan, 2006). There is high absorption and reflectance of clay mineral features in bands 7 and 6 (2.10 – 2.30 μm) according to Traore et al. (2020).

All the band ratios differentiate non-vegetated, vegetated, and urban settlements (Figure 9). However, the RGB band ratio images (6/5 7/6 4/7) in Figure 6 and (5/4 6/5 7/6) in Figure 7 used in this study effectively worked in the granites' lithological discrimination associated rock units. In (5/4 6/5 7/6) Figure 9 (b), the fresh granite appears bluish-green whereas the weathered granites have a red color. This is because weathered surfaces are rich in clay minerals and deficient in plagioclase feldspar (Michalski et al., 2004). The limestone appears yellowish green. The band ratio 6/7 was used for the lithological mapping of clay minerals and kaolinite

due to high and low reflectance. The clay minerals and Fe-rich particles are associated with the limestone porosity.

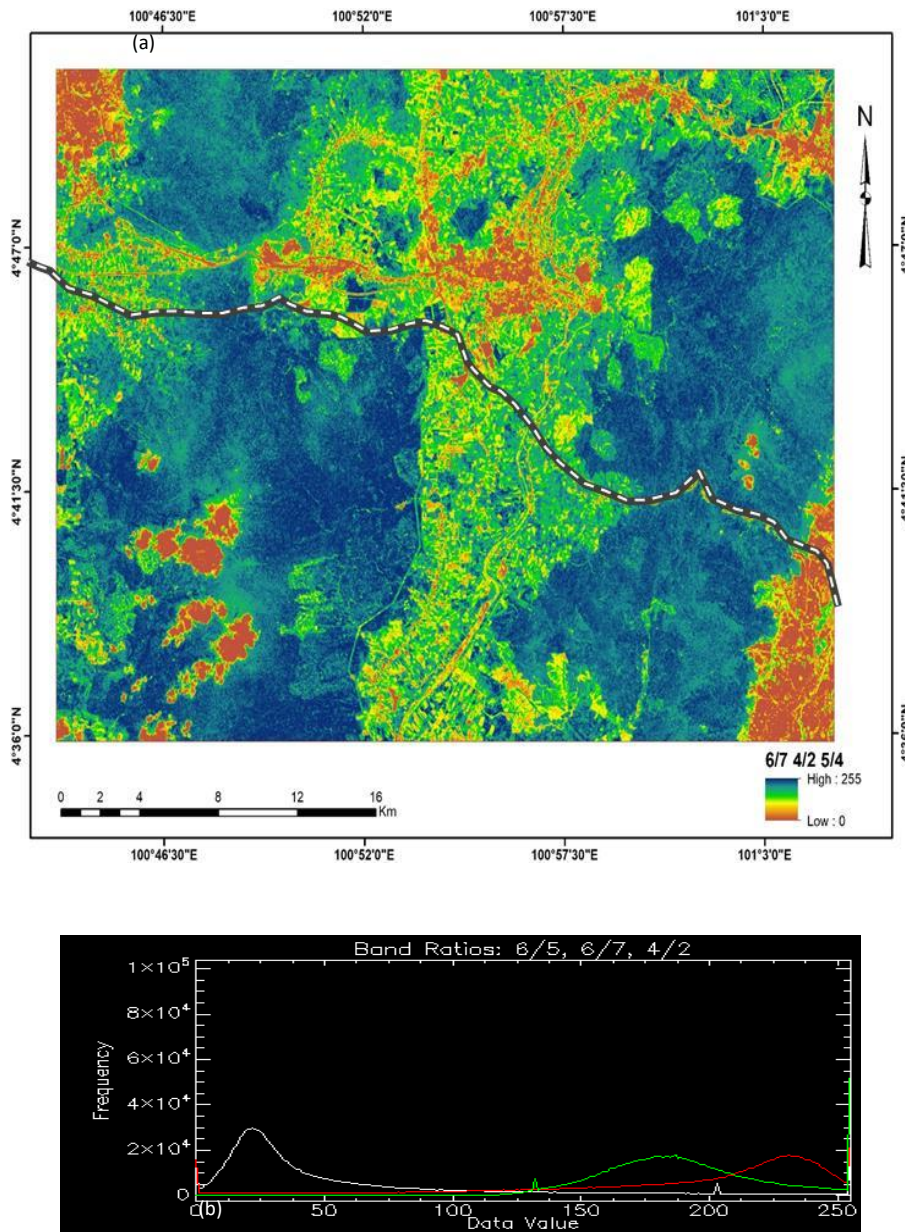


Figure 7. (a) Composite 6/7 4/2 5/4 Bands and (b) Spectral Reflectance

Table 6. The band combination is 6/5, 6/7, 4/2

Basic Stats	Min	Max	Mean	Stdev	Threshold Value	Conf.
B6/B5	0	255	58	60	238	98%
B6/B7	0	255	186	64	250	92%
B4/B2	0	255	192	32	224	92%

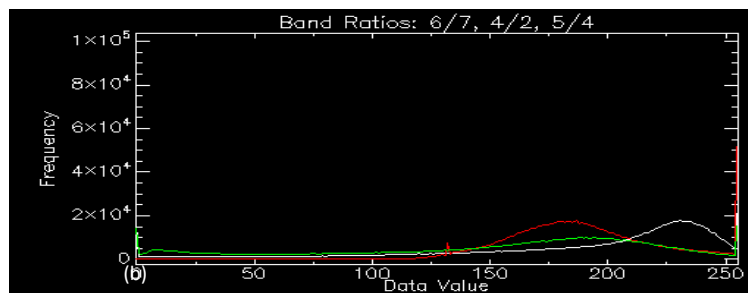
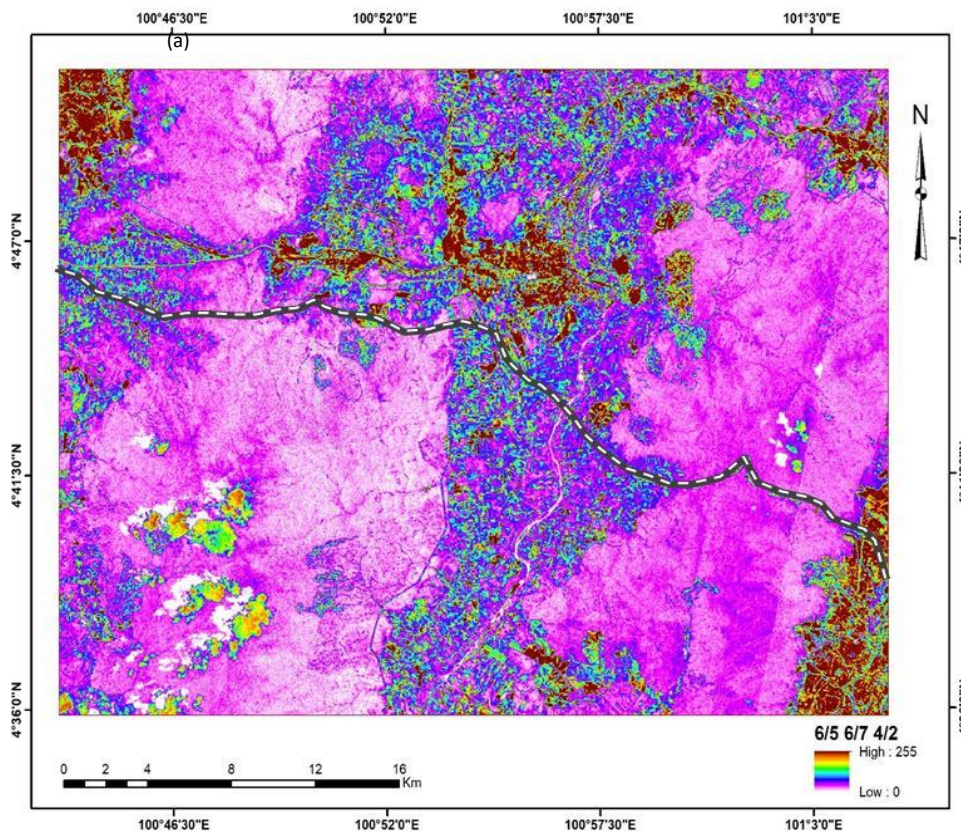


Figure 8. (a) Composite 6/5 6/7 4/2 Bands and (b) Spectral Reflectance

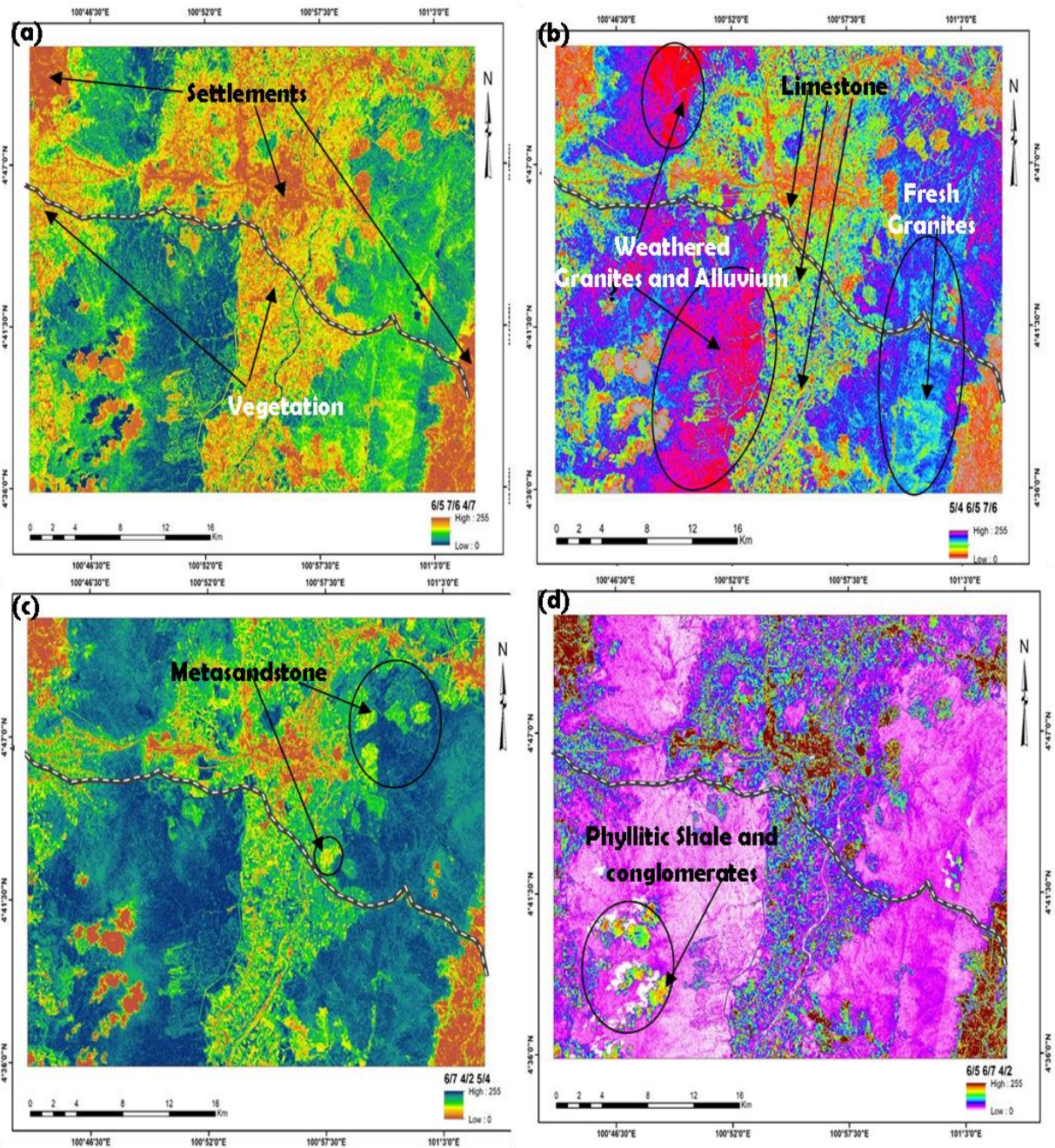


Figure 9. Comparative Analysis of bands (a) 6/5 7/6 4/7, (b) 5/4 6/5 7/6, (c) 6/7 4/2 5/4, (d) 6/5 6/7 4/2.

In band ratio image (6/7 4/2 5/4) Figure 10 (c), the fresh granites do not appear with the weathered granite and are not visible due to the similarity of the spectral colors and tones of lithological units in the different rock formations. Therefore, using only spectral color to separate the rock units for the different rock formations is usually challenging (Dionísio et al., 2009). Alternating layers of clastic rocks, such as shale and mudstone, are seen hidden within the boundary of granites and limestones (6/7 4/2 5/4, Figure 9(c)). In band ratio (6/5 6/7 4/2),

Figure 9 (d), the whitish appearance of weathered sandstone outcrops is seen. The best band ratio combination for the detection of hidden lithologies is therefore observed in 5/4 6/5 7/6, Figure 9 (b) as it depicts almost all the properties of the other combinations, including the distinctive depiction of weathered surfaces that are rich in clay mineral and deficient in plagioclase feldspar. This is because weathering is consistent in such areas due to continuous exposure to rock exfoliation properties such as high precipitation. It is also advisable to integrate several discriminating band ratio images for a successful detailed lithological mapping of granites or other rocks. Discrepancies among ratio maps may help to recognize the strength/weakness of using specific ratios for certain mapping assignments. Calibration and evaluation of resolving power of any band ratio are achieved utilizing other proven ground truth data.

8. Conclusion

The Taiping to Ipoh stretch of the highway, an essential link to cities, is seen to be underlain by different lithologies that are mostly covered by thick vegetation. The application of remote sensing using band ratioing with the integration of geological fieldwork shows the lithological combination as granites, limestones, Phyllites, and metasandstones using band ratios 6/5 7/6 4/7, 5/4 6/5 7/6, 6/7 4/2 5/4, 6/5 6/7 4/2. The best ratio was 5/4 6/5 7/6 illustrating the most distinct spectral reflectance and absorption capability bringing out the hidden lithologies such as weathered medium-grained granites, which are different from the porphyritic granites. In addition to displaying a different spectral response, these combinations also enhance the textural information of the different lithologies, which can also be used to discriminate different rocks. About 90% of the study area is seen to be granitic, which is quite stable when it comes to landslides, but further research will justify it.

Acknowledgements

The authors would like to thank The Department of Petroleum Geoscience Universiti Teknologi PETRONAS and the University at large for the necessary support and assistance to undertake and complete this write up.

References

- Adiri, Z., El Harti, A., Jellouli, A., Maacha, L. and Bachaoui, E.M., 2016. "Lithological Mapping Using Landsat 8 OLI and Terra ASTER Multispectral Data in the Bas Drâa Inlier, Moroccan Anti Atlas". *Journal of Applied Remote Sensing*, 10(1): 016005.
- Ahmad, A.C., Zin, I.N.M., Rosli, M.N., Ab Wahid, A.M. and Kamar, I.F.M., 2016. "Hazard and Risk of Highway Maintenance Works: Case Study of PLUS Expressways". In *MATEC Web of Conferences* (Vol. 66, p. 00106). EDP Sciences.
- Ahmad, L., Shah, M.T. and Khan, S.D., 2016. "Reflectance Spectroscopy and Remote Sensing Data for Finding Sulfide-Bearing Alteration Zones and Mapping Geology in Gilgit-Baltistan, Pakistan". *Earth Science Informatics*, 9(1): 113-121. doi: 10.1007/s12145-015-0239-x.
- As of July 19, 2012, the website USGS accessed "Landsat 8-9 Operational Land Imager (OLI) and Thermal Infrared Sensor (TIRS)." https://www.usgs.gov/faqs/what-are-band-designations-landsat-satellites?qt-news_science_products=0#qt-news_science_
- Askari, G., Pour, A.B., Pradhan, B., Sarfi, M. and Nazemnejad, F., 2018. "Band Ratios Matrix Transformation (BRMT): A Sedimentary Lithology Mapping Approach Using ASTER Satellite Sensor". *Sensors*, 18(10): 3213.
- Available: <https://www.klia2.info/trips/highways/plus-expressway-north-south-expressway/>.
- Balaji, T. and Sumathi, D.M., 2014. "Effective Features of Remote Sensing Image Classification Using Interactive Adaptive Thresholding Method". arXiv preprint arXiv:1401.7743.
- DeGraff, J.V. and Romesburg, C., 1980. "Regional Landslide Susceptibility Assessment for Wildland Management: A Matrix Approach".
- Dionísio, A., Braga, M.A.S. and Waerenborgh, J.C., 2009. "Clay Minerals and Iron Oxides-Oxyhydroxides as Fingerprints of Firing Effects in a Limestone Monument". *Applied Clay Science*, 42(3-4): 629-638.
- Directorate of National Mapping, Malaysia, 1989. "Topographic Map of Kuala Kangsar Sheet 3463," in L7030, K.K. No. 230 - 1986 ed. Malaysia, 1989.
- Directorate of National Mapping, Malaysia, 1989. "Topographic Map of Sungai Siput Utara Sheet 3563."
- Directorate of National Mapping, Malaysia, 2006. "Topographic Map of Ipoh, Sheet 3562."
- Directorate of National Mapping, Malaysia, 2014. "Geological Map of Peninsular Malaysia 9th Edition"

- Fatima, K., Khattak, M.U.K., Kausar, A.B., Toqeer, M., Haider, N. and Rehman, A.U., 2017. "Minerals Identification and Mapping Using ASTER Satellite Image". *Journal of Applied Remote Sensing*, 11(4): 046006.
- Fell, R., Stapledon, D. and Macgregor, P., 2012. "12 Landslides and Geologic Environments". *Landslides: Types, Mechanisms and Modeling*:134.
- Georgiadis, G. A., Tranos, M. D., Makedon, T. K., & Dimopoulos, G. C. 2007. "Contribution of Geological Mapping in Road Construction: An Example from Verta-Kozani National Road, Kastania Area". *Bulletin of the Geological Society of Greece*, 40(4): 1652-1663.
- Gupta, R.P., 2017. "Remote Sensing Geology". Springer.
- Klia2.info. 2019, "PLUS Expressway, North-South Expressway (E1 & E2) " [Online].
- Kockelman, W.J., 1986. "Some Techniques for Reducing Landslide Hazards". *Bulletin of the Association of Engineering Geologists*", 23(1): 29-52.
- Lillesand, T., Kiefer, R.W. and Chipman, J., 2015. "Remote Sensing and Image Interpretation". John Wiley & Sons.
- Mars, J.C. and Rowan, L.C., 2006. "Regional Mapping of Phyllic-And Argillic-Altered Rocks in the Zagros Magmatic Arc, Iran, Using Advanced Spaceborne Thermal Emission and Reflection Radiometer (ASTER) Data and Logical Operator Algorithms". *Geosphere*, 2(3): 161-186.
- Metcalf, I., 2013. "Tectonic Evolution of The Malay Peninsula". *Journal of Asian Earth Sciences*, 76: 195-213.
- Michalski, J.R., Reynolds, S.J., Sharp, T.G. and Christensen, P.R., 2004. "Thermal Infrared Analysis of Weathered Granitic Rock Compositions in the Sacaton Mountains, Arizona: Implications for Petrologic Classifications from Thermal Infrared Remote-Sensing Data". *Journal of Geophysical Research: Planets*, 109 (E3).
- OpenTopography. "SRTM, Raster."
<https://portal.opentopography.org/result?id=rt1592240952626&metadata=1> (accessed 15/06/2020)
- Ourhzif, Z., Algouti, A. and Hadach, F., 2019. "Lithological Mapping Using Landsat 8 Oli And Aster Multispectral Data in Imini-Ounilla District South High Atlas of Marrakech". *International Archives of the Photogrammetry, Remote Sensing & Spatial Information Sciences*.
- Pour, A.B. and Hashim, M., 2015. "Hydrothermal Alteration Mapping from Landsat-8 Data, Sar Cheshmeh Copper Mining District, South-Eastern Islamic Republic of Iran". *Journal of Taibah University for Science*, 9(2): 155-166.

- Sa'adin, S.L.B., Kaewunruen, S. and Jaroszweski, D., 2016. "Risks of Climate Change with Respect to the Singapore-Malaysia High Speed Rail System. *Climate*", 4(4): 65.
- Sautter, B., Pubellier, M., Jousset, P., Dattilo, P., Kerdraon, Y., Choong, C.M. and Menier, D., 2017. "Late Paleogene Rifting Along the Malay Peninsula Thickened Crust". *Tectonophysics*, 710: 205-224.
- The Director General of Mineral and Geoscience Malaysia, 2014. Geological Map of Peninsular Malaysia (9th ed.). Scale 1:750000.
- Traore, M., Wambo, J.D.T., Ndepete, C.P., Tekin, S., Pour, A.B. and Muslim, A.M., 2020. "Lithological and Alteration Mineral Mapping for Alluvial Gold Exploration in the South East of Birao Area, Central African Republic Using Landsat-8 Operational Land Imager (OLI) Data". *Journal of African Earth Sciences*, 170: 103933. doi: <https://doi.org/10.1016/j.jafrearsci.2020.103933>.
- USGS, 2020. "Landsat 8-9 Operational Land Imager (OLI) and Thermal Infrared Sensor (TIRS)." https://www.usgs.gov/faqs/what-are-band-designations-landsat-satellites?qt-news_science_products=0#qt-news_science_products (accessed).
- Yusof, N.M., Pradhan, B., Shafri, H.Z.M., Jebur, M.N. and Yusoff, Z., 2015. "Spatial Landslide Hazard Assessment Along the Jelapang Corridor of the North-South Expressway in Malaysia Using High Resolution Airborne Lidar Data". *Arabian Journal of Geosciences*, 8(11): 9789-9800.